PHYSICAL REVIEW B VOLUME 43, NUMBER 16 1 JUNE 1991

Secondary electrons induced by fast ions under channeling conditions. II. Screening of fast heavy ions in solids

Hiroshi Kudo and Kunihiro Shima
Institute of Applied Physics, University of Tsukuba, Ibaraki 305, Japan

Seiji Seki* and Toyoyuki Ishihara
Tandem Accelerator Center, University of Tsukuba, Ibaraki 305, Japan
(Received 20 February 1990; revised manuscript received 22 October 1990)

Ion-beam shadowing effects have been observed for secondary electrons induced by various ions in the energy range of 1.8–3.8 MeV/amu, under various channeling conditions in Si and GaAs crystals. From a comparison of the energy spectra of electrons induced by ions of equal velocity, we have found reduced shadowing effects for heavy ions (Si, S, and Cl) as compared with light (H, He, C, and O) ions. It is concluded that the reduction results from the screening of the heavy ion's nuclear charge by bound electrons. By analyzing the reduced shadowing effect, the effective nuclear charges for the heavy ions within the target crystals have been determined.

I. INTRODUCTION

When fast ions are incident on solids, an equilibrium charge-state distribution is quickly established as a result of the balance between electron-capture and loss processes.[1] The equilibrium charge-state distributions of fast ions have been measured for various cases by transmission experiments using thin foils.[1–4] Because it affects the balance between capture and loss processes, channeling changes the ion's charge state distribution in transmission experiments with single crystals.[5–8] For example, Martin[5] observed a slight increase of the mean charge for channeled ions compared with the random (nonchanneling) ones in the case of C and O ions of 5.2–35.4 MeV in Si and Ni. On the other hand, Lutz *et al.*[6] observed a decrease for 60-MeV I ions in Au. It was shown[5,6] that channeling experiments provide important information on electron loss and capture processes under restricting conditions for the impact parameters of the collisions.

Ion-beam shadowing, which occurs near the surface under channeling incidence conditions, can be reduced by the presence of the projectile's bound electrons which screen the ion's nuclear charge. Therefore, study of the shadowing effect can provide information on the charge states of the ions. The important aspect of this method is that the charge states within the solid can be measured, which is essentially different from the case of transmission experiments in which the charge state of all emerging ions is measured.

This paper demonstrates the feasibility of a method to determine the charge state of heavy ions in solids using shadowing effects in secondary electrons yields.[9,10] A computer-simulation analysis of the effect of screening on shadowing is also reported.

II. PRINCIPLE OF THE METHOD

In this section we discuss the method to determine from secondary electron spectra measured under channeling conditions the effective nuclear charge of heavy ions in a crystal.

It has been shown in the preceding paper[10] that for equal-velocity ions the electron yield is proportional to the square of the ion's atomic number Z_1. Furthermore, for fully stripped ions incident on a crystal of atomic number Z_2, the flux density of the ions around an atomic row is determined only by a single parameter, i.e., the shadow cone radius, R, given by

$$R=(8Z_1Z_2e^2d/M_1v^2)^{1/2}\ , \tag{1}$$

where M_1 and v are the ion's mass and velocity, respectively, e is the electronic charge, and d is the interatomic distance along the atomic row.[11,9] Consequently, we expect that for a given channeling direction the ratio of the channeling to random electron yield in the keV energy range is the same for equal-velocity ions if they are fully stripped, and have the same Z_1/M_1 value such as ^{2}H (deuterons), ^{4}He, ^{12}C, ^{16}O,. . . , and with a neglecting small difference, also ^{35}Cl.

Since most of the ions undergo only soft collisions with impact parameters larger than the typical inner-shell radius (of the order of 0.1 Å), the ion's nuclear charge is effectively screened when the inner-shell electrons are not removed. Screening reduces the ion-atom interaction, resulting in a reduced shadowing effect compared with the fully stripped case. The reduced shadowing effect can be observed as enhanced ratios of channeling to random yield for heavy ions compared with those for the equal-velocity and fully stripped light ions.

For such soft collisions we introduce the effective nuclear charge Z_{eff}. The reduced shadow cone radius in this case is then given by

$$R=(8Z_{\text{eff}}Z_2e^2d/M_1v^2)^{1/2}\ , \tag{2}$$

instead of Eq. (1).

High-energy (keV) electrons are produced by the ions in close-encounter collisions. Under channeling incidence conditions, the collisions are localized near the

 ©1991 The American Physical Society

surface as a result of the shadowing effect.[9,10] For each axial direction of the crystal, the effective target thickness, i.e., the thickness of the localized region of the collisions is a function of the shadow cone radius R.[9] For close-encounter collisions between inner-shell electrons and fast ions, a simple relationship is empirically obtained by computer simulations: the effective target thickness is proportional to R^{-1}. Such R dependence corresponds to a special case of the universal plot suggested by Feldman,[11,12] for the nuclear encounter probabilities.

The electron yields above the binary-peak energy E_B, i.e., the maximum energy transferable from an ion to a free electron at rest, result from scattered inner-shell electrons only.[9,10] From measurements of the ratio of channeling to random electron yield above E_B, the values of Z_{eff} can be determined. Because of the R^{-1} dependence of the effective target thickness, the effective nuclear charge can be written as

$$Z_{\text{eff}}=(W_f/W_s)^2 Z_1 \;, \tag{3}$$

where W_f and W_s ($\geq W_f$) denote the channeling to random yield ratios for fully stripped light ions and screened heavy ions, respectively.

For the electron yields below the binary-peak energy E_B, which include recoiled valence (or outer-shell) electrons, the R dependence of the effective target thickness is not known since the valence contribution comes not only from the surface region but also from a deep region of the crystal.[10] For electron yields below E_B, the shadowing effect is not properly taken into account in Eq. (3) because the valence electrons, distributed far from the nuclei, are not well shadowed in contrast to inner-shell electrons. Under the extreme assumption that the shadowing effect is absent except for inner-shell electrons, the ratio of channeling to random yield below E_B has a constant contribution approximately equal to the ratio, β, of the number of the valence (or outer-shell) electrons to that of all electrons; for example, $\beta=4/14$ for Si. In this case, Eq (3) must be replaced by

$$Z_{\text{eff}}=[(W_f-\beta)/(W_s-\beta)]^2 Z_1 \;, \tag{4}$$

where W_f and W_s are the corresponding yield ratios below E_B. The actual value of Z_{eff} is expected to lie between the two limiting cases given by Eqs. (3) and (4).

For GaAs, Z_{eff} can be well determined using Eq. (4). We use a value of $\beta=0.166$ in the present analysis, rather than to use $\beta(=4/32)=0.125$ for valence electrons only, since the calculations for 3.75-MeV/amu O ions on GaAs ⟨100⟩ have shown that 16.6% of all electrons (i.e., 5.3 electrons per atom) are not shadowed at the maximum depth of 307 Å contributing to the electron yield at 5 keV,[10] see Fig. 6 in Ref. 10.

III. EXPERIMENTAL

Details of the experiments are similar to those described in the preceding paper.[10] The electron yields both below and above the binary-peak energy were measured in the experiments.

It should be noted that the electron yields for Si and GaAs samples measured under channeling conditions showed no noticeable change during the beam irradiation of doses ranging from 10^{13} to 10^{16} ions/cm^2, even for the heavy Si, S, and Cl ions. The typical beam dose for one spectrum was $10^{14}-10^{15}$ ions/cm^2.

IV. RESULTS AND DISCUSSION

As in the preceding paper,[10] the energy spectra presented do not include any correction for the energy dependence of the spectrometer's acceptance.

A. Spectrum shapes

Figure 1 shows energy spectra of secondary electrons emitted from Si, by impact of 1.875-MeV/amu ^{16}O and ^{32}S ions under ⟨110⟩ channeling and random conditions. The vertical scale represents the electron yield divided by Z_1^2. Similar results are shown in Fig. 2 for the case of GaAs channeling and random incidences. For the ran-

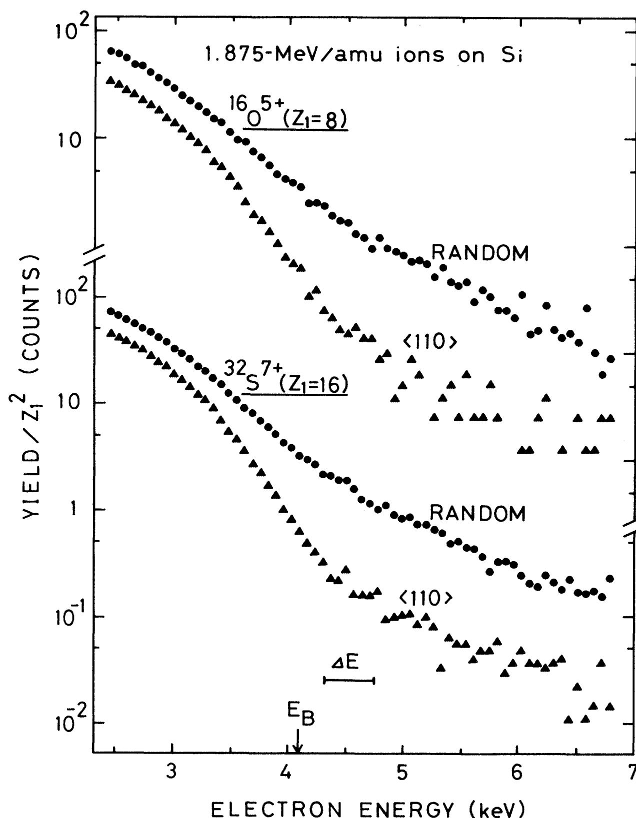

FIG. 1. Energy spectra of secondary electrons induced by 1.875-MeV/amu $^{16}O^{5+}$ and $^{32}S^{7+}$ under Si ⟨110⟩ channeling and random conditions, measured at a backward angle of 180°. The electron yield is normalized to the square of the ion's atomic number Z_1. The spectrometer's energy resolution ΔE, which is proportional to the electron energy, is shown representatively at 4.5 keV. E_B indicates the binary-peak energy (4.1 keV).

dom spectra shown in Figs. 1 and 2, the Z_1^2 scaling, which stems from the binary close-encounter character of the production of recoiled target electrons,[10] is confirmed for the electron yields in the whole energy range below and above E_B, within an uncertainty of about $\pm 20\%$ in the vertical state.

It is seen in Figs. 1 and 2 that the ratio of the channeling to random yield is nearly constant well above E_B (i.e., between 5 and 7 keV) and well below E_B (i.e., between 2.5 and 3.5 keV). The same behavior is also seen in Fig. 3 which shows the electron spectra measured for 3.75-MeV/amu $^{16}O^{8+}$ ($E_B = 8.2$ keV) incident in the ⟨100⟩ channeling or random directions of Si and GaAs crystals.

B. Observation of the reduced shadowing effect

To demonstrate the anticipated enhancement of the ratio of the electron yields for Si and GaAs crystals, we have collected several series of data using 3.75-MeV/amu (equal-velocity) beams of $^2H^+$, $^4He^{2+}$, $^{10}B^{4+}$, $^{10}B^{5+}$, $^{12}C^{4+}$, $^{12}C^{6+}$, $^{16}O^{6+}$, $^{16}O^{8+}$, $^{28}Si^{13+}$, $^{28}Si^{14+}$, $^{32}S^{10+}$, $^{32}S^{15+}$, and $^{35}Cl^{11+}$. We have also used 2.5- and 2.8-MeV/amu beams of $^{12}C^{4+}$, $^{16}O^{5+}$, $^{16}O^{6+}$, $^{28}Si^{7+}$, $^{32}S^{7+}$, and $^{35}Cl^{8+}$.

It should be noted first that for the ions used the ratios of channeling to random yield do not depend within an uncertainty of about $\pm 5\%$ on the initial charge state of the incident ions. This indicates that the ions have reached their equilibrium charge state distribution.

Figure 4 shows the measured yield ratios, W_0, below E_B for Si ⟨110⟩, ⟨100⟩, and ⟨310⟩ incidences of the 3.75-MeV/amu ions. While W_0 is constant for light ions ($Z_1 \leq 8$), it is larger for heavy ions ($Z_1 \geq 14$). Figure 5 shows similar results for GaAs ⟨100⟩. The energy ranges, for which the values of W_0 are determined for GaAs, are 4.0–6.0 keV for 3.75-MeV/amu ions, and 3.3–3.7 keV for 2.5- and 2.8-MeV/amu ions. Also, for GaAs an enhancement of W_0 for the heavy ions is observed.

A similar enhancement is also measured for the electron yield above E_B, where the electron yield results only from close-encounter recoils of tightly bound inner-shell electrons in the target. Table I summarizes the measured yield ratios, W_1, above E_B for 1.875- and 3.75-MeV/amu O^{8+} and S^{15+}. We can see that, once again, almost all values of W_1 for ^{32}S ions are larger than those for ^{16}O ions.

C. Determination of Z_{eff}

From the reduction in the shadowing effect for heavy ions, the effective nuclear charge of those ions in the solid

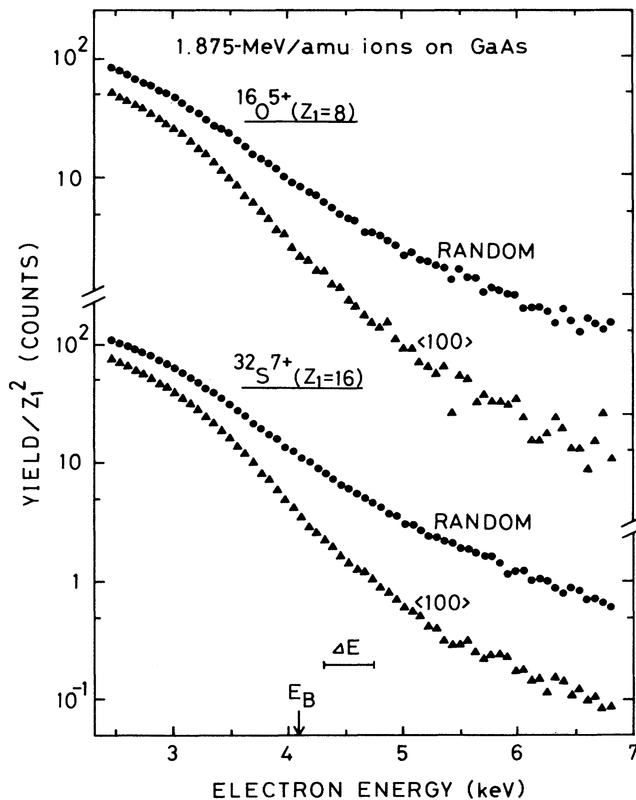

FIG. 2. Energy spectra of secondary electrons induced by 1.875-MeV/amu $^{16}O^{5+}$ and $^{32}S^{7+}$ under GaAs ⟨100⟩ channeling and random conditions.

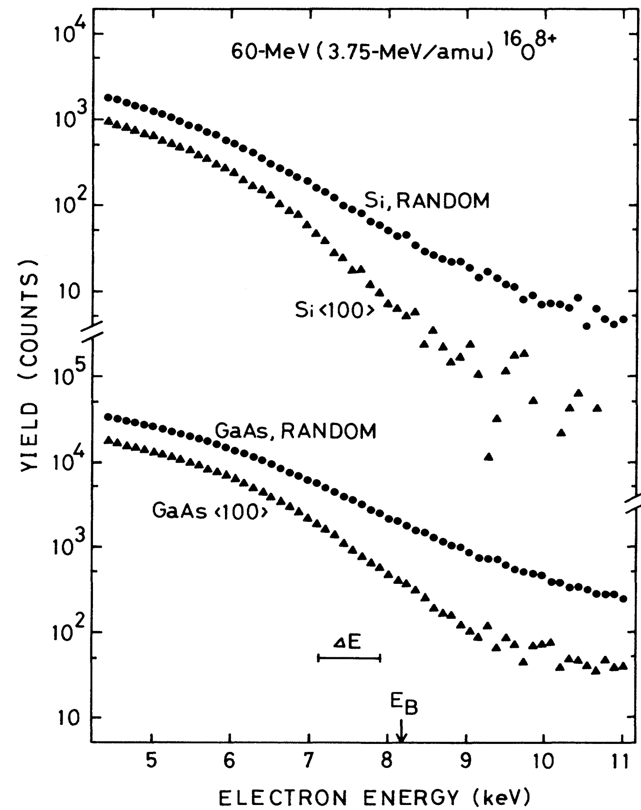

FIG. 3. Energy spectra of secondary electrons induced by 3.75-MeV/amu $^{16}O^{8+}$ under ⟨100⟩ channeling and random conditions in Si and GaAs crystals. The binary-peak energy E_B (=8.2 keV) is indicated.

TABLE I. Values of W_1, the ratio of channeling to random electron yield above the binary-peak energy E_B, obtained from the measurements for 1.875- and 3.75-MeV/amu ^{16}O and ^{32}S ions. The uncertainty in the values is roughly $\pm 10\%$. The energy range in the spectra, over which W_1 was determined is denoted in parentheses for each case.

(1) 1.875 MeV/amu (E_B=4.1 keV)	^{16}O	^{32}S
Si ⟨110⟩ (4.8–6.2 keV)	0.073	0.12
GaAs ⟨100⟩ (5.5–6.8 keV)	0.11	0.15
(2) 3.75 MeV/amu (E_B=8.2 keV)	^{16}O	^{32}S
Si ⟨110⟩ (9.0–10.5 keV)	0.054	0.067
Si ⟨100⟩ (9.0–10.5 keV)	0.070	0.11
Si (100) (9.0–10.5 keV)	0.29	0.35
GaAs ⟨110⟩ (9.2–11.0 keV)	0.13	0.12

can be determined, as discussed in Sec. II. We first discuss the analysis using the yield ratios W_0 (below E_B).

For the ratio for fully stripped ions, W_f, in Eqs. (3) and (4) we take the average value of W_0 for the light ions shown in Figs. 4 and 5. We obtain for 3.75-MeV/amu ions W_f=0.38, 0.50, 0.60, for Si ⟨110⟩, Si ⟨100⟩, and Si ⟨310⟩, respectively, and W_f=0.46 for GaAs ⟨100⟩. Similarly, W_f=0.56 for the 2.5- and 2.8-MeV/amu ions for GaAs ⟨100⟩. This procedure is reasonable since transmission measurements of the ion's charge states have shown that the mean charges Q of light ions ($Z_1 \leq 8$ in this case) are close to the values of Z_1. For example, $Q \simeq 5.9$ and 7.7 for 3.75-MeV/amu C and O ions in C foils, respectively, and $Q \simeq 5.7$ for 2.5- and 2.8-MeV/amu C ions in C foils.[3] By using the above-mentioned values of W_f, Z_{eff} for the heavy ions in the channeling cases follows from Eqs. (3) or (4), where we take W_s equal to W_0 for the heavy ions.

Figure 6 shows the results for the 3.75-MeV/amu ions

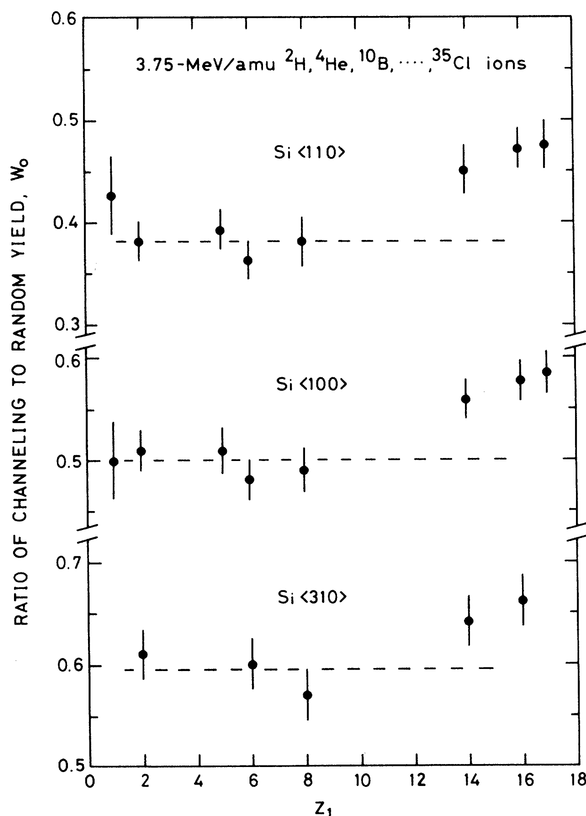

FIG. 4. Z_1 dependence of the channeling to random electron yield ratio W_0 for 4–6 keV secondary electrons emitted under Si ⟨110⟩, ⟨100⟩, and ⟨310⟩ channeling conditions of the 3.75-MeV/amu various ions. The dashed lines indicate the ratios for the light ions.

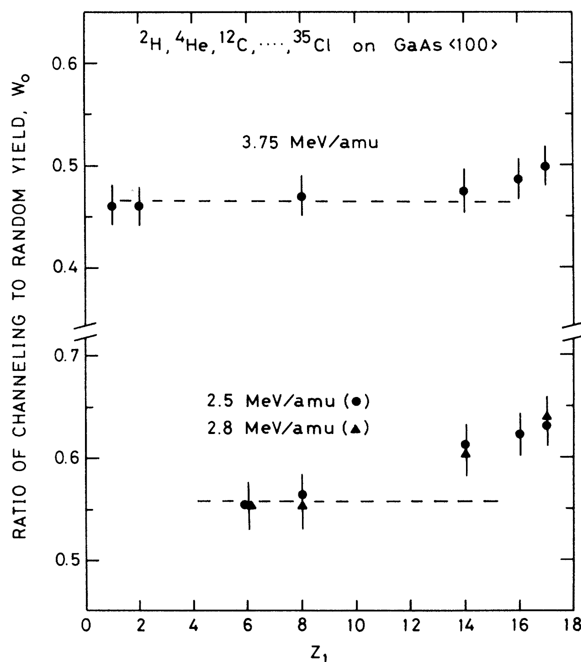

FIG. 5. Z_1 dependence of the channeling to random yield ratio W_0 for secondary electrons emitted under GaAs ⟨100⟩ channeling conditions of various 2.5-, 2.8-, and 3.75-MeV/amu ions, shown similarly to Fig. 4. The dashed lines indicate the ratios for the light ions.

under various channeling conditions in Si. The uncertainty in Z_{eff}, about ± 1, stems from the uncertainty in the values for W_0. The difference $Z_1 - Z_{eff}$ should correspond to the number of bound electrons in the inner shells of the ion. In Fig. 6, the values of Z_{eff} determined from Eq. (4) are unrealistic because for ⟨110⟩ $Z_1 - Z_{eff}$ exceeds 10, the total number of K- and L-shell electrons. This is not consistent with the assumption that screening is due to K- and L-shell electrons only. Z_{eff} determined from Eq. (3) is lower for stronger channeling directions: 13.0, 12.1, and 10.5 for S ions for Si ⟨310⟩, Si ⟨100⟩, and Si ⟨110⟩ cases, respectively. Therefore, it may be expected that Z_{eff} for random incidence should be higher than for ⟨310⟩. It is noted that the mean charges of 3.75-MeV/amu S and Si ions passed through Al foils are 13.6 and 12.3, respectively.[13,14,3]

Figure 7 shows the results for 3.75-, 2.8-, and 2.5-MeV/amu ions for GaAs ⟨100⟩ channeling. As noted in Sec. II for the GaAs case the analysis based on Eq. (4) is more realistic than to use Eq. (3), although the use of Eq. (3) or Eq. (4) does not lead to very different values for Z_{eff}. It is reasonable that the difference between Z_1 and Z_{eff} obtained does not exceed 10. The values of Z_{eff} for 3.75-MeV/amu ions [curve (a)] are larger than those for 2.8- and 2.5-MeV/amu ions [curve (b)] by about 1.8. This qualitatively corresponds to the energy dependence of the ion's mean charge observed in transmission experiments; for example, the mean charges of 3.75- and 2.5-MeV/amu S ions passed through C foil are 14.3 and 13.3, respectively.[3]

The values of Z_{eff} for the S ions can also be determined from the values of W_1 measured for the S and O ions, summarized in Table I, assuming also that the O ions are fully stripped at 3.75 MeV/amu and are in the charge state of 7+ at 1.875 MeV/amu (the mean charge after passing through C foil[3]). As shown in Figs. 6 and 7 for a few cases, the values of Z_{eff} obtained from W_1 is consistent with those from W_0 although the uncertainty is large (about ± 2.5); for Si they lie between the two limiting cases determined using W_0, and for GaAs the value of $Z_{eff} = 7.5$ for the 1.875-MeV/amu ions indicates the trends that Z_{eff} decreases with decreasing ion velocity. It should be noted that in the channeling case the recoiled electrons are produced mainly by the ions running near the atomic rows (i.e., near the regions with a high-density of electrons). Therefore, it is mainly the charge state of these ions that is measured, in contrast to the case of transmission experiments in which the charge state of all emerging ions is measured.

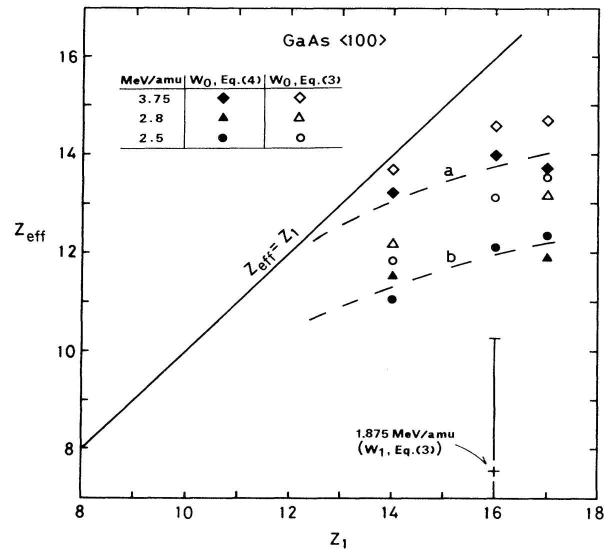

FIG. 7. Z_{eff} plotted against Z_1 for 3.75-, 2.8-, and 2.5-MeV/amu ions under GaAs ⟨100⟩ channeling condition. The results obtained by using Eq. (3) are shown for comparison (open symbols). The result obtained from the yield ratios W_1 (above E_B) for 1.875-MeV/amu ions is also shown. The dashed curves are drawn to guide the eye for the 3.75-MeV/amu ions (a), and for both of the 2.8- and 2.5-MeV/amu ions (b). The estimated uncertainty in Z_{eff} is about ± 1, unless otherwise shown.

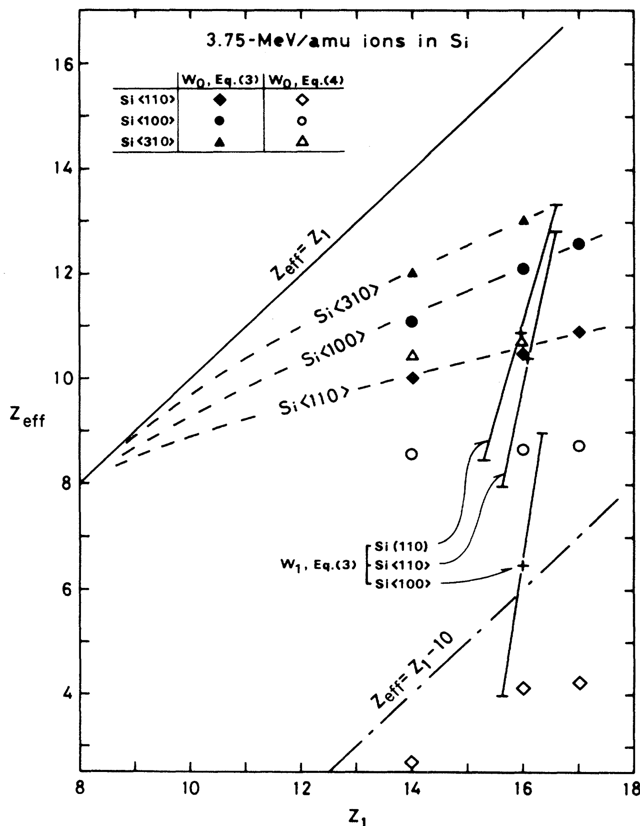

FIG. 6. Effective nuclear charges of the ions, Z_{eff}, plotted against the ion's atomic number Z_1, determined for 3.75-MeV/amu ions in Si under various channeling conditions. The results obtained from the yield ratios W_1 (above E_B) are also shown. The dashed curves are drawn to guide the eye for Z_{eff} obtained by using the yield ratios W_0 (below E_B) for W_f or W_s in Eq. (3). The estimated uncertainty in Z_{eff} is about ± 1, unless otherwise shown. Note that $Z_1 - Z_{eff}$ should correspond to the number of bound electrons in the inner shells of the ion.

D. Modified screening length for the ion-atom potential

Screening of the nuclear charge causes the reduction of the interaction potential between a fully stripped ion and an atom. Therefore, it is of fundamental importance to investigate whether the observed reduced shadowing effect can be explained by a reasonable reduction of the screening length for the most commonly used interaction potential. For this purpose, the approach in terms of the screening length for the Molière potential[8] (Molière approximation to the Thomas-Fermi potential) has been followed.

In the Molière potential, the screening length a_1 for a fully stripped ion and an atom depends only on the atomic number of the atom (Z_2):

$$a_1 = 0.8853 a_0 Z_2^{-1/3} , \quad (5)$$

where a_0 ($=0.529$ Å) is the Bohr radius. For a pair of neutral atoms, the Molière potential is still a good approximation if the parameter a_1 is simply replaced by

$$a_2 = 0.8853 a_0 (Z_1^{1/2} + Z_2^{1/2})^{-2/3} , \quad (6)$$

as suggested by Firsov.[15,8] The trajectories of the ions are mainly determined by collisions with impact parameters of the order of 0.1 Å. Therefore, the shadowing effect for ions that have filled inner shells but no electrons in the outer shells must be the same as that for neutral projectiles and, consequently, their screening lengths should be equal.

To obtain the dependence of the channeling yield on the screening length, computer simulations of the multistring type have been carried out. It is assumed that the impact-parameter dependence of the probability of close-encounter collisions is proportional to the two-dimensional electron density of the target atoms.[10] Details of the simulations have been described elsewhere.[10,16,11]

Figure 8 shows the encounter probability for Si ⟨110⟩, calculated for close-encounter collisions of 3.75-MeV/amu ^{16}O ions with $L_{2,3}$-shell electrons in Si for reduced screening lengths of $0.4a_1$, $0.6a_1$, as well as a_1. The distribution of the L-shell electrons was obtained from numerical tables for atomic wave functions given by Fischer.[17] It is seen in Fig. 8 that the shadowing effect reduces by decreasing the screening length, i.e., by reducing the repulsive force exerting on the ions. The effective target thickness is obtained by integrating the probability from the surface to the depth of about 400 Å.

Figure 9 shows the effective target thickness thus obtained for various electronic shells in Si as a function of the screening length for 3.75- and 1.875-MeV/amu ions under Si ⟨110⟩ and ⟨100⟩ channeling conditions, as well

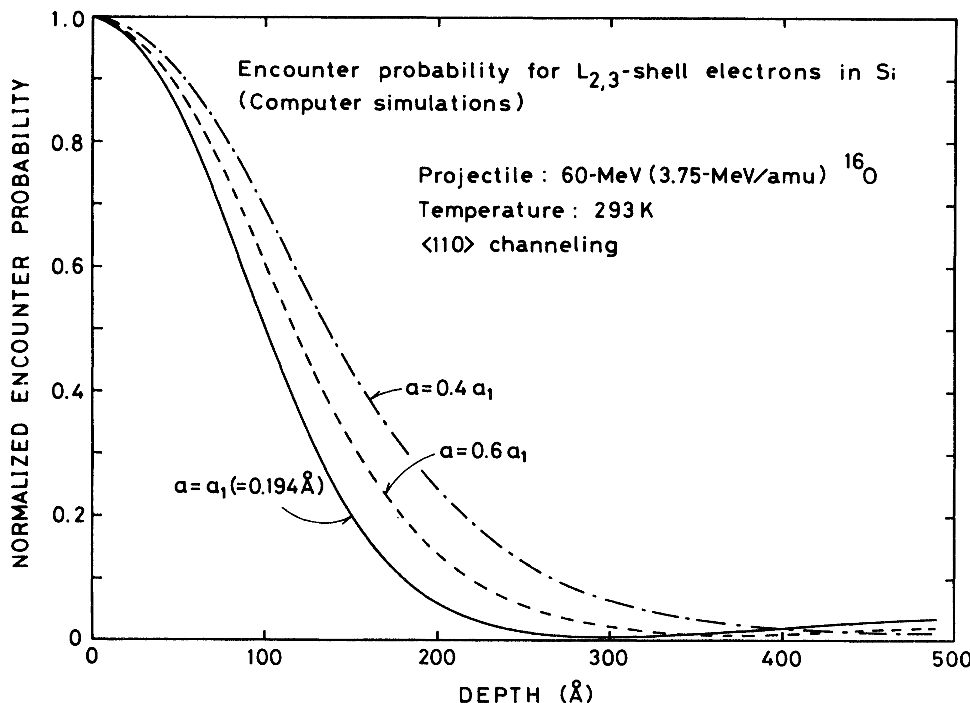

FIG. 8. Dependence of the normalized encounter probability for Si $L_{2,3}$-shell electrons on the screening length of the Molière potential, a, calculated for Si ⟨110⟩ incidences of 3.75-MeV/amu ^{16}O ions.

as for L ($L_1+L_{2,3}$) shell in GaAs for ⟨100⟩ case. For Si atoms, the values of a_2 for Si, S, and Cl ions are 0.122, 0.120, and 0.118 Å, respectively, about 40% less than a_1 (0.194 Å). As seen in Fig. 9, this difference in screening length causes an enhancement of the effective target thickness for both Si ⟨110⟩ and Si ⟨100⟩ cases by about 10 and 15 % for K- and L-shell electrons, respectively, compared with the values calculated for a_1. A similar enhancement (about 10%) is seen for the L shell in GaAs for which the value of a_2 for S ions is 30% less than a_1 (=0.147 Å). The effective target thickness for the L shell is more sensitive to the screening length than that for the K shell because the ion trajectories for different values of the screening length diverge from each other only at large distances to the atomic rows.

Since the valence electrons of Si are less localized near the atomic centers, we expect that the contribution of the valence electrons to the enhancement of the effective target thickness is less than that of the L-shell electrons.

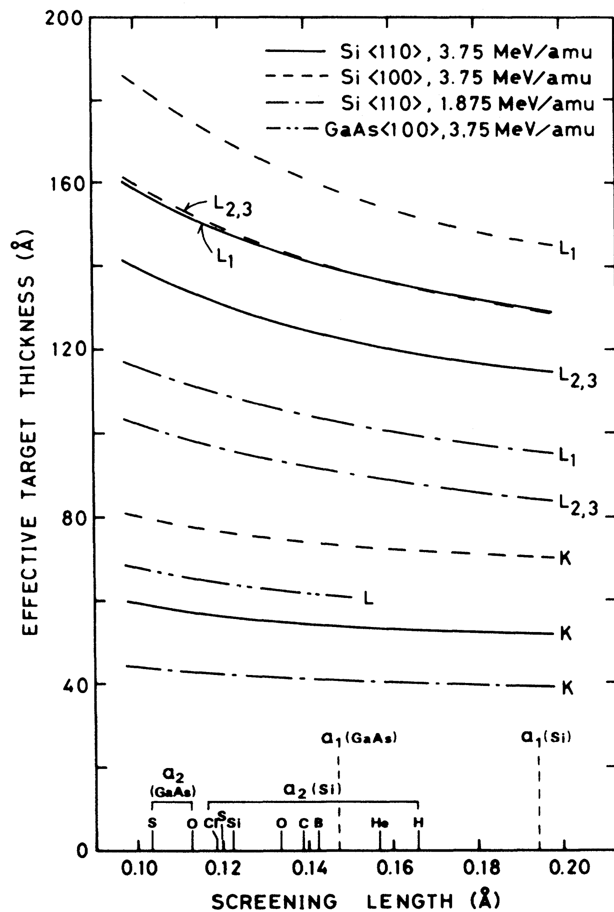

FIG. 9. Effective target thickness for various electronic shells in Si, as well as the L shell in GaAs, as a function of the screening length of the Molière potential, calculated for ⟨110⟩ and ⟨100⟩ channeling incidences of the 1.875- and 3.75-MeV/amu ions. The values of a_1 and a_2 for various ions are indicated.

However, the calculated increase (typically by 15%) of the effective target thickness for the Si L-shell electrons is slightly less than the measured enhancement of W_0 (20%, which includes the valence contribution) for the heavy ions, see Fig. 4. Moreover, the calculated increase (15%) is appreciably less than the enhancement of W_1, more than 24% (Table I) for the Si axial cases. Similarly, for GaAs the enhancement of W_0 for all electrons must be less than that for the inner-shell electrons. However, the calculated increase in the effective target thickness for the GaAs L-shell electrons (by 9% for the present velocity range of the ions) is again less than the observed enhancement of W_0, 13%, for the 2.5- and 2.8-MeV/amu ions. This trend probably indicates that the simulations are only approximately correct, although they are useful for the present purpose.

From the analysis here, we conclude that the observed increase in secondary electron yield under channeling conditions of heavy ions as compared to light ions can be interpreted in terms of a reduction of the screening length in the Molière potential.

Thus, the analysis has shown the applicability of the Firsov screening length [Eq. (6)] to partially stripped ions. It is demonstrative to compare the screening for the heavy ions with that for O ions since they have nearly equal a_2 (see Fig. 9). However, for the channeled 3.75-MeV/amu O ions, the Molière screening length [Eq. (5)] must be used since they are almost fully stripped (Sec. IV C). In contrast, the channeled heavy ions with the same velocity have several electrons (Figs. 6 and 7); and, although they are not neutral, the analysis here suggests that the Firsov screening length (for neutral projectiles) is applicable. The presence or absence of outer-shell electrons is unimportant in the interaction between an ion and the atoms in the crystal, as mentioned earlier in this section.

V. CONCLUDING REMARKS

The present work has demonstrated that the measurement of high-energy secondary electrons under channeling conditions can provide unique information on the charge states of ions within solids.

The charge states determined by the present method is probably characteristic of the heavy ions that pass through the dense electron region along the vicinity of the atomic rows. The charge states of fast ions under such conditions have never been measured by transmission experiments. Extensive measurements under various channeling conditions should provide experimental data useful for the study of the dependence of charge state on the interatomic distance, i.e., on the collision interval.

ACKNOWLEDGMENTS

We thank the staff members of Tandem Accelerator Center, University of Tsukuba, for their assistance in the experiments.

*Present address: ULVAC Corporation, Kanagawa 253, Japan.

[1]H. D. Betz, Rev. Mod. Phys. **44**, 465 (1972).

[2]H. D. Betz, in *Methods of Experimental Physics,* edited by L. Marton and C. Marton (Academic, New York, 1980), Vol. 17, Chap. 3.

[3]K. Shima, T. Mikumo, and H. Tawara, At. Data Nucl. Data Tables **34**, 357 (1986).

[4]K. Shima, N. Kuno, and M. Yamanouchi, Phys. Rev. A **40**, 3557 (1989).

[5]R. W. Martin, Phys. Rev. Lett. **22**, 329 (1969).

[6]H. O. Lutz, D. Datz, C. D. Moak, and T. S. Noggle, Phys. Lett. **33A**, 309 (1970).

[7]S. Datz, F. W. Martin, C. D. Moak, B. R. Appleton, and L. B. Bridwell, Radiat. Eff. **12**, 163 (1972).

[8]D. S. Gemmell, Rev. Mod. Phys. **46**, 129 (1974).

[9]H. Kudo, K. Shima, S. Seki, K. Takita, K. Masuda, K. Murakami, and T. Ipposhi, Phys. Rev. B **38**, 44 (1988).

[10]H. Kudo, K. Shima, K. Masuda, and S. Seki, preceding paper, Phys. Rev. B **43**, 12 729 (1991).

[11]L. C. Feldman, J. W. Mayer, and S. T. Picraux, *Material Analysis by Ion Channeling* (Academic, New York, 1982).

[12]L. C. Feldman, Nucl. Instrum. Methods **191**, 211 (1981).

[13]U. Scharfer, C. Henrichs, J. D. Fox, P. Von Brentano, L. Degener, J. C. Sens, and A. Pape, Nucl. Instrum. Methods **146**, 573 (1977).

[14]K. Shima, T. Ishihara, T. Momoi, T. Miyoshi, K. Numata, and T. Mikumo, Phys. Lett. **98A**, 106 (1983).

[15]O. B. Firsov, Zh. Eksp. Teor. Fiz. **33**, 696 (1957) [Sov. Phys. JETP **6**, 534 (1958)].

[16]H. Kudo, D. Schneider, E. P. Kanter, P. W. Arcuni, and E. A. Johnson, Phys. Rev. B **30**, 4899 (1984).

[17]C. Froese Fischer, At. Data **4**, 301 (1972).